JOURNAL OF MATERIALS SCIENCE: MATERIALS IN MEDICINE 8 (1997) 227–232

Fabrication of hydroxyapatite ceramic with controlled porosity

DEAN-MO LIU
Materials Research Laboratories, Industrial Technology Research Institute, Chutung, Hsinchu,Taiwan 31015

Porous hydroxyapatite (HAp) ceramics were fabricated using poly vinyl butyral (PVB) as a porosifier. The effects of preparation conditions involving PVB particle size, sintering time, and forming pressure (die-pressing technique) on the resultant pore size/structure as well as the pore size distribution were investigated. The experimental results showed that the HAp ceramics with controlled pore characteristics such as pore volume fraction, pore size and pore structure are achievable. It provides the possibility to design HAp ceramics with diverse porosities simulating that of natural bone.

1. Introduction

Hydroxyapatite (HAp) and related calcium phosphate (CP) materials have been widely used as implant materials for many years due to their close similarity in composition and high biocompatibility with natural bone [1, 2]. Recently, a number of reports have emphasized the fabrication and properties of porous HAp or CP ceramics [3–5]: attention is particularly placed on the influence of pore size on bone ingrowth behaviour [6, 7]. These porous bioactive materials are currently used for bone repair and augmentation. Many *in vivo* studies have revealed the significance of the porous structure of the biomaterials on the promotion of bone ingrowth [7–9]. However, as indicated by Hulbert *et al.* [10], macropores of at least 100 μm are needed to host the cellular and extracellular components of bone and blood vessels, and greater than 200 μm are expected to be effective in osteoconduction.

Therefore, control of porosity within the porous HAp/CP ceramics is an important subject for many investigations. Recently, a novel technique in the fabrication of porous HAp ceramics has been conducted by impregnating a cellulose spongy body with interconnected macropores (>150 μm) into a HAp-contained slurry, followed by heat treating to drive off the spongy body and to densify the ceramic powder [3]. A resulting HAp ceramic with a replica spongy structure is obtained. This technique allows the fabrication of HAp with an open-pore structure and permits the use of spongy bodies of diverse porosities to simulate the natural bone structure. However, the strengths of these replica HAp are relatively low and this may restrict possible load-bearing clinical applications. More recently, Arita *et al.* [11] obtained porous HAp ceramic sheets by means of a tape casting technique with $CaCO_3$ as a gas-forming agent. HAp ceramic sheets with highly porous microstructure (up to 62%) were successfully developed but the pore size is limited to only several micrometres.

This study aims at developing porous HAp ceramic with controlled porosity using poly vinyl butyral (PVB) particles of different size fractions as a porosifier. The influence of sintering time, forming pressure and PVB particle size on the resultant pore characteristics of the porous HAp ceramic were investigated.

2. Materials preparation

2.1. HAp powder synthesis

Reagent-grade $Ca(OH)_2$ and H_3PO_4 were employed (each of which was dissolved in deionized water into a solution of 1.0 M) to form a precipitate by a titration method in a vigorously-stirred container. The solution was kept at $pH = 9.0$ by ammonia hydroxide. The precipitate was collected at various reaction periods followed by oven drying at 200 °C. After 24 h reaction, the precipitate was granulated by a spray dryer to form granules near spherical in shape and ~ 100 μm in diameter. The powders obtained were examined by X-ray diffraction (XRD, Philips PW1700) with CuK_α radiation at a scanning speed of 0.01°/s, Fourier transform infrared spectrometry (FTIR, Bomem, DA3.003), and transmission electron microscopy (TEM, Jeol 400). The Ca/P ratio of the powders was determined by using induced couple plasma-atomic emission spectrometer (ICP-AES, Spectro, Spectroflame-P). An accuracy of better than 3% was verified by a standard solution.

2.2. Porous HAp ceramic preparation

Poly vinyl butyral (PVB) particles with size fractions of 0.093 mm, 0.188 mm and 0.42 mm were used as a porosifier. Powder mixtures containing the HAp granules and 42–61% in volume of PVB particles

0957–4530

were prepared. Five g of the mixed powders were die-pressed uniaxially at pressures of 27 MPa and 55 MPa to form rectangular blocks. The blocks were then heat-treated to 500 °C at a heating rate of 0.5 °C/min to drive off the PVB particles and other volatiles, followed by an increase to 1200 °C for 2 to 48 h for densification purposes.

The porosity of the as-sintered HAp ceramics was determined by mercury porosimetry (Autopore II, 9220). Three to four specimens were selected to determine porosity with an error of less than 1% of the measured porosity value. The pore size and pore structure of the ceramics was examined using scanning electron microscopy (Cambridge Instrument, S360).

3. Results and discussion

3.1. Characteristics of synthetic HAp powders

The powder obtained by the precipitation method has a needle-like shape (Fig. 1) with ~9 nm diameter and 0.1–0.3 μm length. The XRD analyses of the powders for various reaction periods are shown in Fig. 2, together with the values of Ca/P ratio. The powders illustrate increasing Ca/P values from 1.5 to 1.67 for reaction periods from 1 h to 12 h. During the first several hours of reaction the powder precipitates as a mixture of HAp, β-tricalcium phosphate (β-TCP) and small amounts of tetracalcium phosphate (TeCP). After a sufficient maturing period, e.g. 12 h, the powder shows a crystallographic structure closely resembling that of hydroxyapatite (JCPDS, #9-432) and the Ca/P ratio of the powder is 1.67, which is identical to that of stoichiometric HAp. The broad peak width of the diffraction pattern may be attributed to the influence of the powder size.

Fig. 3 illustrates the IR spectra of the powders after different periods of reaction. It is found that the IR spectra of the powder after 12 h reaction show an identical pattern to that of commercial HAp (Amdry 6021, Alloy Metals Inc.). The spectra mainly consisted of two types of vibration; three PO_4^{3-} stretching modes at 960, 1040 and 1080 cm^{-1} bands and two PO_4^{3-} bending modes at 571 and 601 cm^{-1} bands, which match the spectra reported in the literature for the HAp phase [12]. The broad OH^- stretching band around 3570 cm^{-1} suggests the adsorption of H_2O molecules. In addition, a small peak at 1400 cm^{-1} band indicates the presence of a small amount of CO_3^{2-} ions which originate primarily from air during the preparation. This finding implies that the synthetic apatite is of carbonate-contained HAp, which is beneficial for biomedical purposes because of its similarity to bony apatite.

3.2. Fabrication of porous HAp ceramics

The influence of PVB particle size on the resulting porosity of the HAp ceramics sintered at 1200 °C for 2 h is shown in Fig. 4 (the error bars in the figure refer to the minimum and maximum porosity measured), where the values in parentheses denote the volume

Figure 1 TEM photo of the synthetic HAp powders.

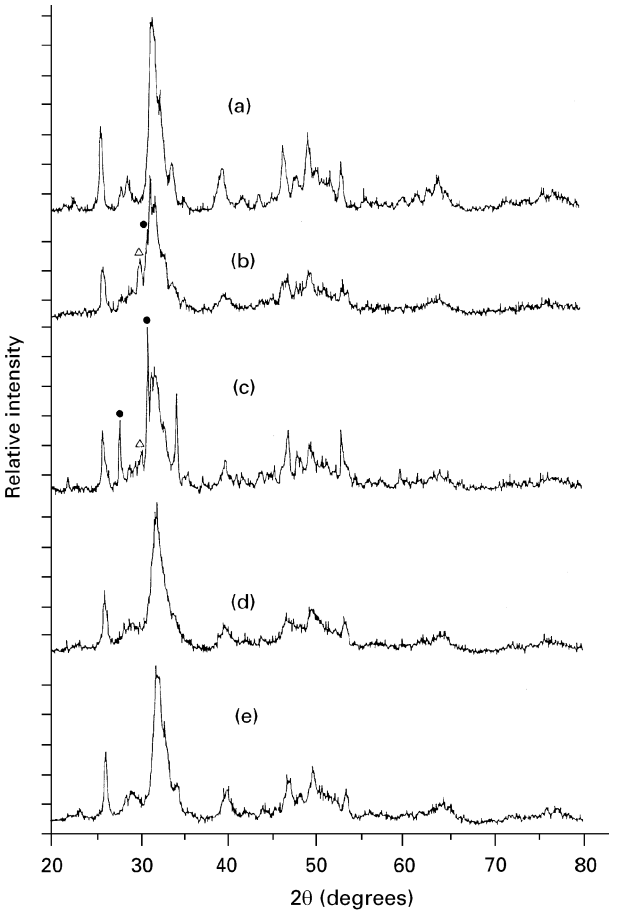

Figure 2 XRD patterns of the powders after different reaction times: (a) 12 h, Ca/P = 1.67; (b) 5 h, Ca/P = 1.62; (c) 3 h, Ca/P = 1.58; (d) 2 h, Ca/P = 1.53; (e) 1 h, Ca/P = 1.50. ● β-TCP; △ TeCP.

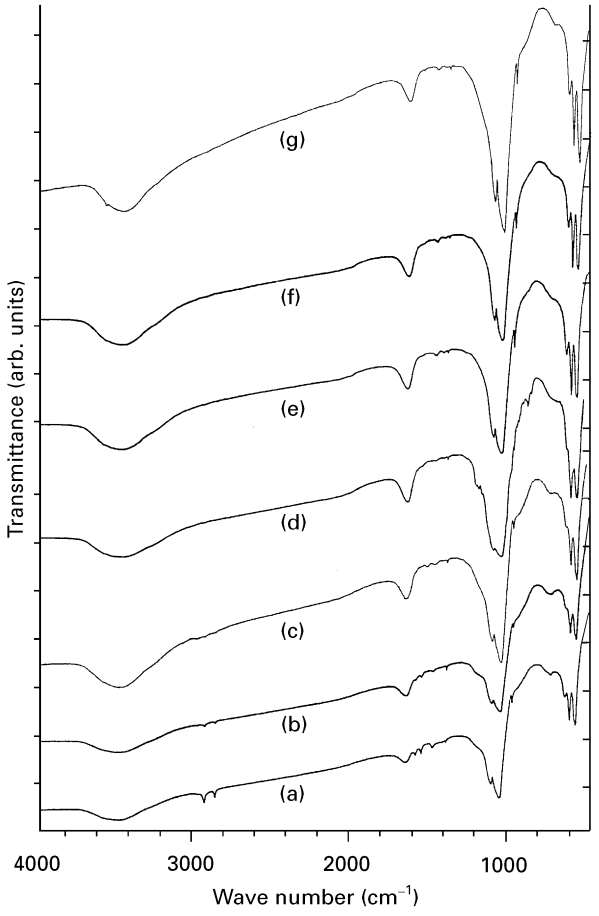

Figure 3 Infrared spectra of the powders after various reaction times (a) 1 h; (b) 2 h; (c) 3 h; (d) 5 h; (e) 12 h; (f) 24 h and (g) the spectra of the commercial HAp for comparison purposes.

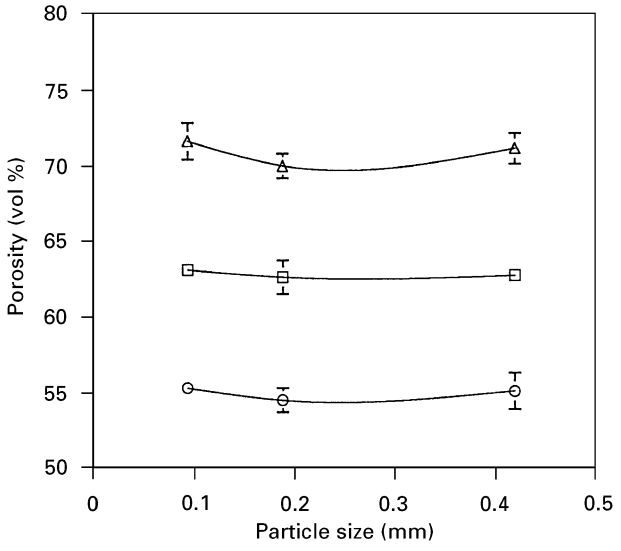

Figure 4 Effect of PVB particle size on the final porosity of the porous HAp ceramics sintered at 1200 °C for 2 h (○ 42%; □ 55.2%; △ 61%).

fraction of PVB phase initially introduced and expected to form the pore phase after high-temperature sintering. It is noted that for a given fraction of PVB, the resulting porosity of the ceramic is roughly independent of the PVB particle size and is higher than the calculated porosity by ~10–12%. If the pore size derived from the original PVB is referred to as "macropore", the additional porosity volume is believed to be due to microporosity as representatively shown in Fig. 5, where the pore size ranges from 1–5 μm. The presence of such microporosity is a result of incomplete densification, as frequently observed in the sintering of polycrystalline ceramics. Therefore, it is possible to achieve a more precise control of macropore characteristics by controlling only PVB particles with diverse morphologies if the microporosity can be eliminated significantly or completely. To accomplish this, a higher compaction pressure, i.e. 55 MPa, was employed. The resulting porosity with respect to the introduced PVB volume fraction is shown in Fig. 6. The powder mixture consolidated at 55 MPa yields a less porous body at a given PVB content compared to that consolidated at 27 MPa. This is reasonable because the HAp powders among the PVB particles are expected to be consolidated more densely at higher compaction pressure and this promotes the removal of microporosity within the solid walls. At 55 MPa, the sintered HAp ceramic shows a pore volume fraction similar to that of the PVB volume content initially

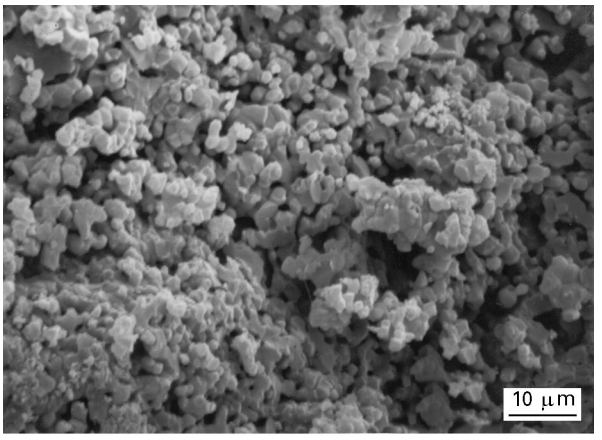

Figure 5 Micropores within the solid walls of the porous HAp ceramic.

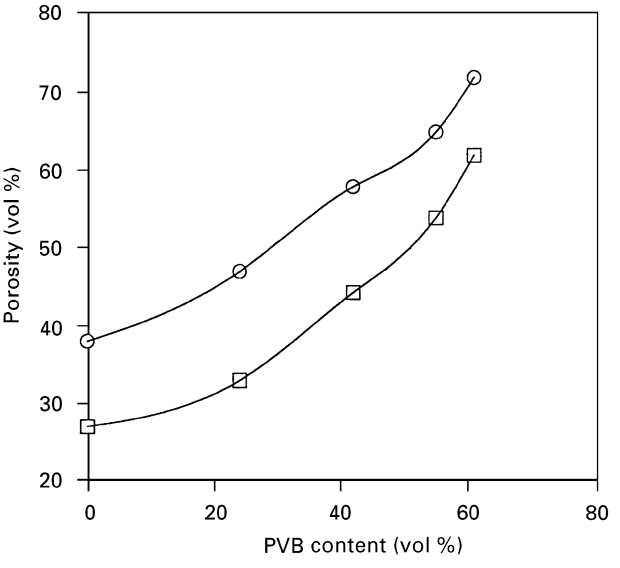

Figure 6 Measured porosity versus corresponding PVB volume fraction introduced at a compaction pressure: ○ 27 MPa; □ 55 MPa.

introduced. This suggests the elimination of microporosity. Further analysis of the pore size distribution by mercury porosimeter is given in Table I for 61 vol % of 0.42 mm PVB particles. The volume fraction of the macropores increases at 55 MPa and confirms the preceding assumption regarding the compaction effect. Fractured surface observation of the porous HAp specimen is shown in Fig. 7a, and in 7b at a larger magnification. The pores are essentially interconnected and the pore shape is nearly spherical (a few of them show ellipsoidal geometry) and is similar to the shape of the PVB particle. The pore sizes can generally be categorized as $\sim 360\,\mu m$, $\sim 15\,\mu m$ and 2 μm.

An alternative approach to densify the solid walls is by extension of sintering time. Two types of PVB particle of different sizes, with 55.2% and 61% volume fractions, were employed. Figs 8a and b show the resulting porosity after different sintering periods for 0.188 mm and 0.42 mm PVB, respectively. At the lower forming pressure, considerable densification continues for sintering times up to 10 h; however, further extensive sintering does not promote the removal of microporosity to any significant extent. Instead, the porosity of the ceramics tends to remain constant, with a value greater by approximately 1–2 vol % than the calculated porosity. In comparison, the densification behaviour appears to be independent of the PVB size. When increasing the forming pressure to 55 MPa, the change in porosity with sintering time is limited (see closed circles in Fig. 8a), the resulting porosity of the HAp ceramics is close to the calculated porosity and the measured value is sustained even after 30 h of sintering. This may be attributed to the complete elimination of microporosity, leaving only the pore phase originated from the starting PVB particles. An SEM photo of the fractured

TABLE I Pore size distribution of the sintered porous HAp ceramics at various compaction pressures and sintering time periods (pore sizes smaller than 5 μm are defined as "micropores" and those larger than 5 μm as "macropores")

Compaction pressure (MPa)	Total porosity (vol %)	Microporosity (%)	Macroporosity (%)
27 (2 h)	71	39	32
55 (2h)	61.6	24.7	36.4

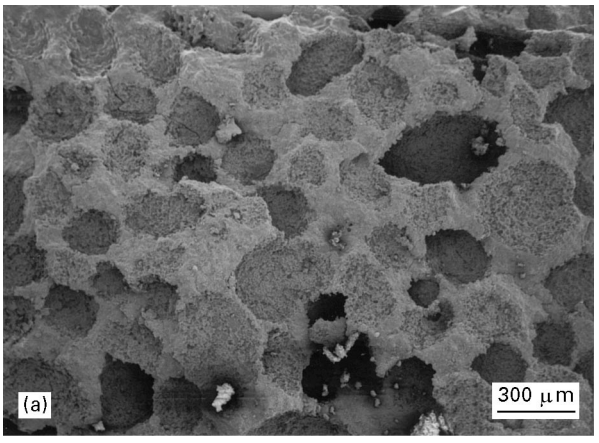

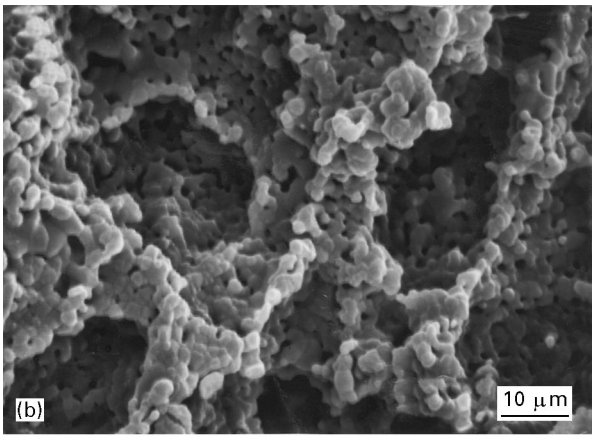

Figure 7 Scanning electron micrographs of the fractured surface of the ceramic (0.42 mm PVB particles) (a) at a low magnification and (b) a detailed examination of the solid wall microstructure.

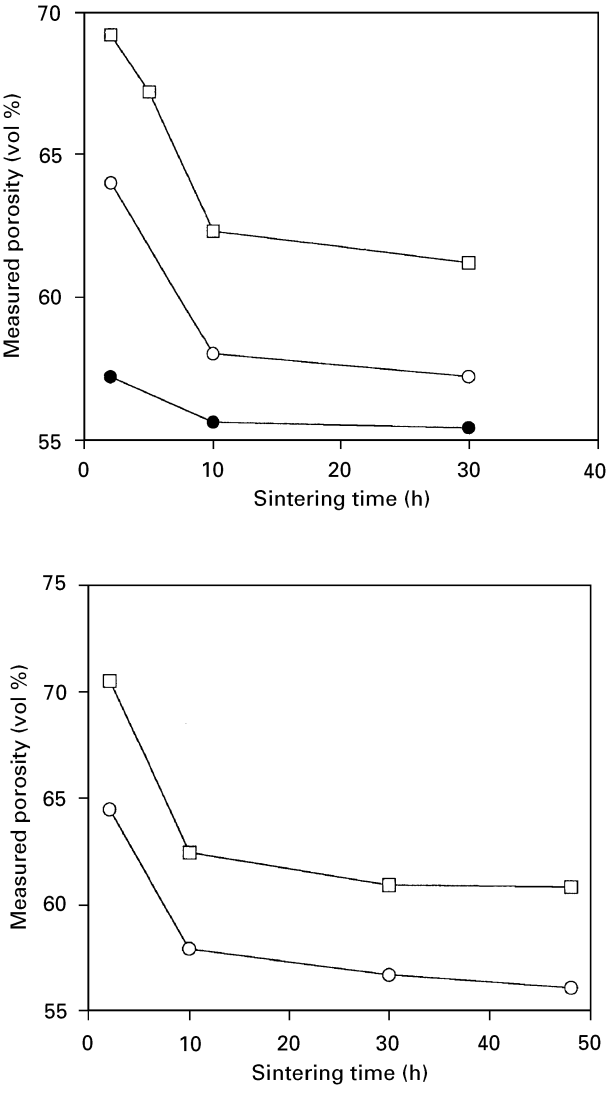

Figure 8 Effect of sintering time (sintering temperature 1200 °C) on the resulting porosity of the porous HAp ceramics with starting (a) 0.188 mm and (b) 0.42 mm PVB particles of different volume fractions. (a) □ 27 MPa, 61 vol %; ○ 27 MPa, 55.2 vol %, ● 55 MPa, 55.2 vol %. (b) □ 27 MPa, 61 vol %; ○ 27 MPa, 55.2%.

surface of the specimen prepared at 55 MPa and sintered at 1200 °C for 30 h is shown in Fig. 9, revealing that the microstructure of the solid walls seems to be much denser than that of the sample sintered for 2 h (Fig. 7a).

One interesting finding is that the macropores created by the PVB particles have an average pore size which varies with sintering period. After direct measurement of the macropore size of over 70 pores of each type of PVB particle in terms of sintering period, Fig. 10 shows the resulting relation between average macropore size (AMS) and sintering time. Macropore shrinkage by ~10% in size is observed for each PVB size during the first few hours of sintering and this may be attributed to the densification effect, particularly for such ultra-fine HAp crystallites. This macropore shrinkage corresponds to a total volume reduction of the initial PVB phase of ~27%. Therefore, the effective macropore volume is reduced to, for example, 45% for an initial 61 vol % of PVB phase. Further sintering shows little influence on macropore shrinkage suggesting that an equilibrium macropore size with respect to the sintering temperature is reached. In association with the porosity changes previously discussed in Fig. 8, prolonged sintering time does promote the elimination of microporosity within the solid walls to a significant extent, but not completely. An SEM observation of a solid wall for the ceramic (~55.2% porosity) sintered for 30 h is shown in Fig. 11, where micropores (1–5 μm in size), with volume fraction calculated to be ~15% (i.e. 55.2×0.27), are easily seen. The calculated micropore volume is close to the value determined by the mercury porosimeter, i.e. 16.6%. The similarity in microporosity of the calculated and measured values suggests that the micropores within the solid walls are essentially of open structure, accessible to mercury penetration. Interconnected micropores are important to allow the flow of body fluid between the macropores, e.g. the supply of nutrition, and subsequently promote the growth of hard tissue into the macropores [8].

To ascertain the properties of the sintered ceramics, XRD analysis was employed and the diffraction pattern of the sintered porous ceramics reveals a typical HAp crystal structure as shown in Fig. 12. EDAX analysis through SEM examination shows no impurity other than Ca or P elements present, Fig. 13. Further study of porous HAp ceramics as implant materials for bone replacement is currently in progress and will be reported shortly.

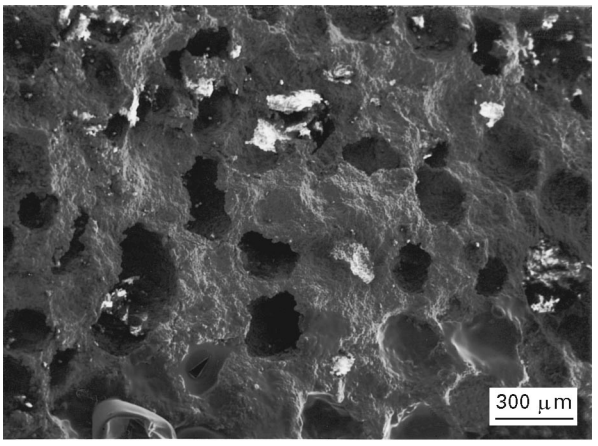

Figure 9 Fractured surface of the porous HAp sintered at 1200 °C for 30 h.

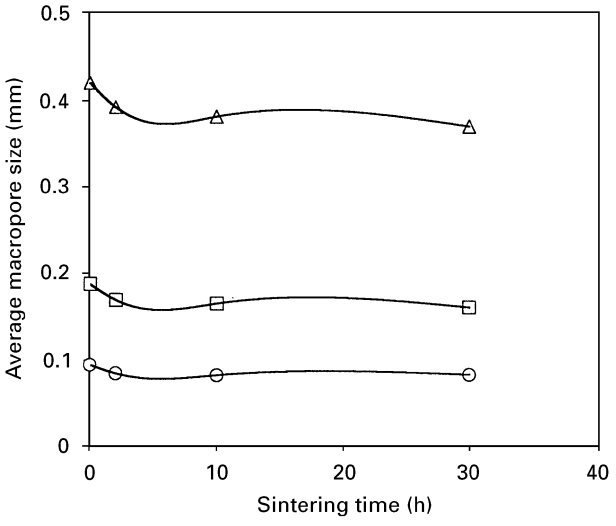

Figure 10 Effect of sintering time on the average macropore size of the porous HAp ceramics: ○ 0.093 mm; □ 0.18 mm; △ 0.42 mm.

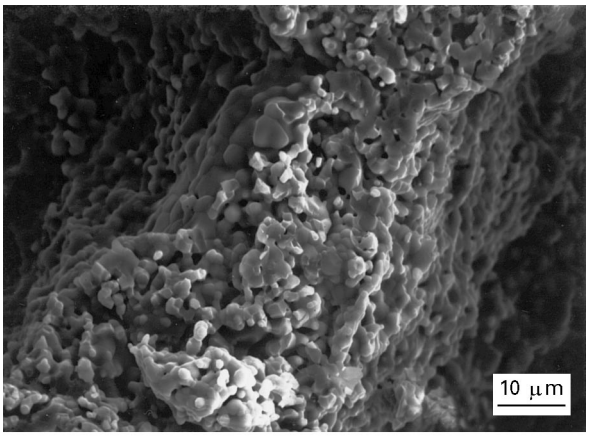

Figure 11 Scanning electron micrograph of the solid wall microstructure, ceramic sintered for 30 h.

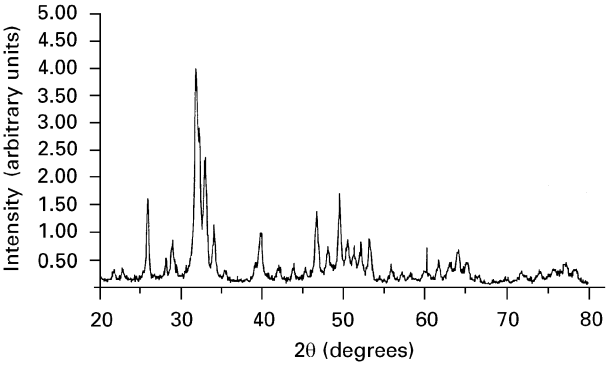

Figure 12 XRD patterns of the sintered porous ceramic, typical of HAp crystal structure.

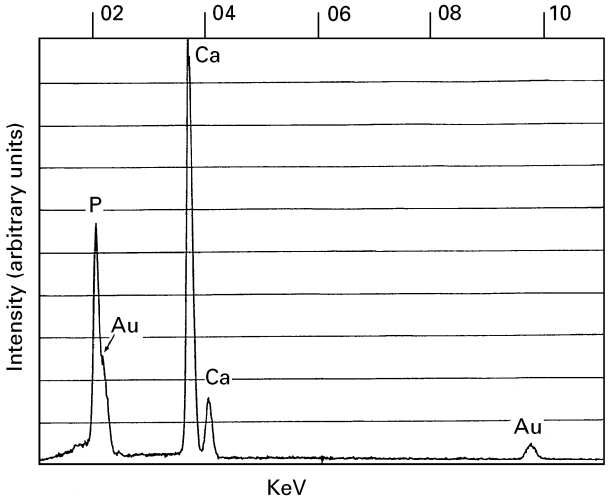

Figure 13 EDAX of the sintered HAp ceramic showing that no impurity other than Ca and P is present. The Au is sputtered-coated for SEM purposes only.

4. Conclusion

Fine, needle-like hydroxyapatite (HAp) crystallites with an atomic ratio Ca/P = 1.67 were synthesized using a precipitation method. The porous HAp ceramics were successfully fabricated with controlled pore characteristics such as pore size, pore shape, and pore size distribution, by the incorporation of 42–61% by volume of poly vinyl butyral (PVB) particles of different size fractions, i.e. 0.093 mm, 0.188 mm and 0.42 mm. Forming pressure (die-pressing technique) and sintering time (at a fixed temperature of 1200 °C) were found to play important roles in the control of microporosity within the solid walls, and hence the pore size distribution. Macropores show a size reduction of approximately 10% compared to the PVB particle size initially introduced and reach an equilibrium size after prolonged sintering. Therefore, it is possible to fabricate porous HAp ceramics with diverse pore structures simulating that of living bone by means of the present technique.

Acknowledgements

The author thanks the Ministry of Economic Affairs, Taiwan, for funding this research under contract No. 843CF4130.

References

1. K. DE GROOT, *Biomaterials* **1** (1980) 47.
2. V. JASTY, M. JARCHO, K. L. GUMAER, R. SANER-SCHELT and H. P. DROBECK, 9th International Congress Electron Microscopy **2** (1978) 674.
3. M. FABBRI, G. C. CELOTTI and A. RAVAGLIOLI, *Biomaterials* **16** (1995) 225.
4. I. H. ARITA, D. S. WILKINSON, M. A. MONDRAGON and V. M. CASTANO, *ibid.* **16** (1995) 403.
5. K. IOKU, S. SOMIYA and M. YOSHIMURA, *J. Mater. Sci. Lett.* **8** (1989) 1203.
6. H. OHASHI, M. THERIN, A. MEUNIER and P. CHRISTEL, *J. Mater. Sci. Mater. Med.* **5** (1994) 237.
7. B. A. RAHN, J. NEFF, A. LEUTENEGGER, R. MATHYS and S. M. PERREN, in "Biological and biomechanical performance of biomaterials", edited by P. Christel, A. Meunier and A. J. C. Lee (Elsevier Science Publishers, Amsterdam, 1986) pp. 21–26.
8. W. CHEN, X. ZHANG, J. WANG and X. ZHAO, in "Biomedical Materials Research in the Far East", edited by X. Zhao and Y. Ikada (Kobunshi Kankokai, Tokyo, 1993) pp. 157–158.
9. G. DALCUSI and N. PASSUTI, *J. Biomed. Mater. Res.* **11** (1990) 86.
10. S. F. HULBERT, S. J. MORRISON and J. J. KLAWITTER, *J. Biomed. Mater. Res. Symp.* **2** (1970) 269.
11. I. H. ARITA, V. M. CASTANO and D. S. WILKINSON, *J. Mater. Sci. Mater. Med.* **6** (1995) 19.
12. J. ZHOU, X. ZHANG, J. CHEN, S. ZENG and K. DE GROOT, *ibid.* **4** (1993) 83.

Received 17 May 1995
and accepted 18 September 1996